M. Okutan*, Z. Yalçın, O. İçelli, F. Ay, R. Boncukçuoğlu, O. Artun and D. Delipınar

Electrical Behavior of Probertite by Dielectric Spectroscopy

Abstract: In this work of the material investigation, electrical parameters, which are real part and imaginary part of modulus, dielectric constant, dissipation factor, and conductivity, in the bulk pellet of probertite sample is presented. Electrical properties were investigated via temperature and frequency dependent dielectric spectroscopy. Real and imaginary part of dielectric parameter properties of the probertite were measured at frequencies from 100 to 15M Hz in the temperature range of 25 to 150 °C. Temperature dependence of the real part of the dielectric constant suggests that these compounds exhibit strong electromagnetic absorption and broadband electrical behavior.

Keywords: probertite, dielectric spectroscopy, electrical modulus, dissipation factor, boron clay

PACS® (2010). 77.22.Gm, 41.20.Gz

***Corresponding author: M. Okutan:** Department of Physics, Yıldız Technical University, Istanbul, Turkey. E-mail: mokutan@gmail.com
Z. Yalçın, O. İçelli, D. Delipınar: Department of Physics, Yıldız Technical University, Istanbul, Turkey
F. Ay: Department of Mechanical Engineering, Nigde University, Nigde, Turkey
R. Boncukçuoğlu: Department of Environmental Engineering, Atatürk University, Erzurum, Turkey
O. Artun: Department of Physics, Bülent Ecevit University, Zonguldak, Turkey

1 Introduction

Concrete is one of the most common construction materials. Additives play an essential role in modifying properties of concretes [1] and it is one of the most important materials used for radiation shielding in facilities containing radioactive sources and radiation generating equipment [2]. It has many properties desirable from a nuclear radiation shielding point of view. These properties can be changed to suit special shielding needs [3]. The concrete shielding properties may vary and are dependent on the composition of the concrete. Different types of special concretes have been developed by changing the contents used for preparing concrete, depending on the available natural and artificial local materials [4–7]. Probertite which is used in the concrete and cement is glassy and colorless original boron mineral. Turkey is one of the world's leading producers of boron minerals and has the world's largest boron reserves. These minerals are used to produce boron concentrates by removing gangue minerals. Boron concentrates are either directly used in an application area or processed into a more refined boron product [8]. In this work the main concern will be on electromagnetic absorption property of probertite, is a Boron mineral, in concrete. On the other hand, electrical properties, which are electric modulus, dissipation factor, conductivity, and dielectric constant those are dependent on frequency and temperature are investigated according to their chemical composition and concentration (Table 1).

2 Experimental

2.1 Sample preparation

Probertite, which has a specific gravity of 2.14 g/cm^3, crystal structure monoclinic, hardness (mohs) of 3.5, has the formula of $CaNa[B_5O_7(OH)_4]\cdot 3H_2O$ which has the same

Table 1: Chemical composition of probertite.

Element	Concentration (%)	Analyte	Compound formula	Concentration (%)
Al	0.307	Na	Na_2O	8.976
Ca	34.423	Mg	MgO	1.236
Cl	0.084	Al	Al_2O_3	0.311
Fe	0.273	Si	SiO_2	1.510
K	0.095	S	SO_3	0.121
Mg	1.393	Cl	Cl	0.045
Na	12.446	K	K_2O	0.061
O	22.727	Ca	CaO	25.773
Rb	0.022	Fe	Fe_2O_3	0.209
S	0.091	Rb	Rb	0.012
Si	1.320	Sr	SrO	5.856
Sr	9.254	B	B_2O_3	55.89
B	17.565			

B_2O_3, Na_2O and CaO content with ulexite. As seen in Table 1, probertite consists of 55.89% B_2O_3 and 8.976% Na_2O and 25.773% CaO. The materials used in the study were collected from Eti Holding Borax and Acid Factories in Bandirma, Turkey. The samples were dried at 105 °C temperature, then crushed and ground. The particle size of probertite has not been taken into account since it has a crushable structure and completely sieved in 100 mesh-sieves. After the material preparation processes, the sample was pelletized for 15 min and compressed into pellet for 10 seconds with a hydraulic press at a pressure of 122 (Pa) $\times 10^5$. The resulting pellets had 1 mm thickness and 13 mm diameter. The presence of phases in probertite was confirmed by X-Ray diffraction. Thus, in addition to the identification of the principal mineral phases, all materials' analysis consists of conventional X-Ray diffraction analysis. In the next step, XRD peaks of the all materials were compared with the JCPDS files and XRD patterns of randomly oriented powders. They were analyzed by means of "MDI Jade 7 Software". The MDI Jade 7 Software results were provided with mineral structural formula, trace element distributions over minerals, the individual minerals, etc.

2.2 Experimental procedure

The measurement of probertite samples which is sandwiched between two pieces of Au electrode were repeatedly performed by applying different frequencies under different temperatures. The probertite sample was characterized with dielectric spectroscopy to determine its electrical properties. A HP 4194a impedance analyzer was employed in the dielectric spectroscopy measurements. The RMS amplitude of the signal was set to ~500 mV and the temperature dependent complex impedance was measured at logarithmic frequencies between 100 and 15M Hz. The temperature was measured by a PT 100 resistor that is in direct thermal contact with the probertite sample. The Novotherm Temperature Control System (NTCS) enabled the monitoring of the temperature in the 25 to 150 °C range with an accuracy >0.1 °C. It is seen that a frequency sweep at a fixed temperature requires very long time. At each temperature point, the temperature and frequency dependence of the real and imaginary parts of the electrical parameters were recorded by the automated NTCS setup. The surface morphology of the sample was analyzed using atomic force microscopy (AFM, Nano Scope IV, Scanning Probe Microscope Controller).

3 Results and discussion

AFM images of the probertite are shown in Fig. 1a–c. The surface roughness, RMS of the ceramic is 72.732 nm and the maximum height difference on the surface $R_{max.}$ is 356.67 nm (Fig. 1a). The surface roughness reflected in the height of profiles of the images and the surface distributions of the probertite are shown Fig. 1b–c. The parameters of surface morphology of the probertite are presented on figures. AFM images indicate that morphology of surface has irregular structure. The grain size is seen irregularly in a 10×10 μm flatten view (Fig. 1c).

One of the important techniques to characterize many of the electrical and electrochemical properties of fast ionic conductors is the conductivity spectroscopy [9–11]. In general, conductivity measurements are made by applying the DC bias across the material, but it results in the polarization at the electrode-electrolyte interface, which opposes the applied field and hence, the ionic current falls with time. To overcome this problem, the four-probe or two reversible electrode methods are adopted to measure DC conductivity of the materials [10]. Later, the single frequency measurements are carried out, but these methods are found to be inadequate for understanding the complete electrical behavior of the materials, since the electrochemical processes represented by various individual elements (R, C and L) are frequency dependent [12, 13]. Hence, the AC technique has been developed to measure impedance over a range of frequencies to estimate the exact bulk conductivity and frequency dependent conductivity in Fast Ionic Conductors (FICs). From the impedance study, one can obtain not only the bulk conductivity but also grain boundary effects, ionic transport, double layer formation at the electrode/electrolyte interface, etc. Hence, in recent years, Impedance Spectroscopy (IS) has become a powerful technique for characterizing the electrical properties of the FIC materials and their interfaces with electronically conducting electrodes. Also, the IS measurements can provide the dynamic properties to understand the microscopic nature of the FIC materials [10, 12, 14]. The admittance and permittivity are parallel functions characteristic at low frequencies whereas the impedance and modulus are series functions at high frequencies [9, 12]. The complex plane is used to represent the electrical quantities of real and imaginary parts of complex impedance (Z^*), complex permittivity (ε^*) and complex modulus (M^*) [13, 14]. The frequency dependent complex dielectric permittivity is given by

$$\frac{\left(\varepsilon^* - \varepsilon_\infty\right)}{\left(\varepsilon_s - \varepsilon_\infty\right)} = \frac{1}{\left(1 + j\omega\tau\right)} \tag{1}$$

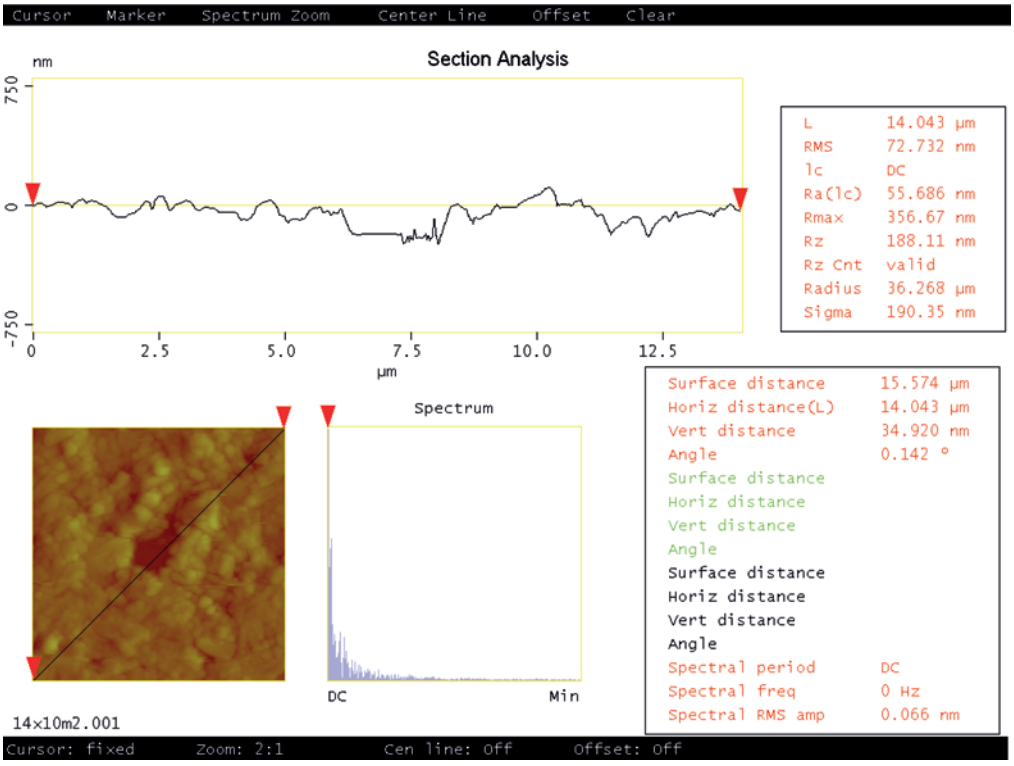

(a)

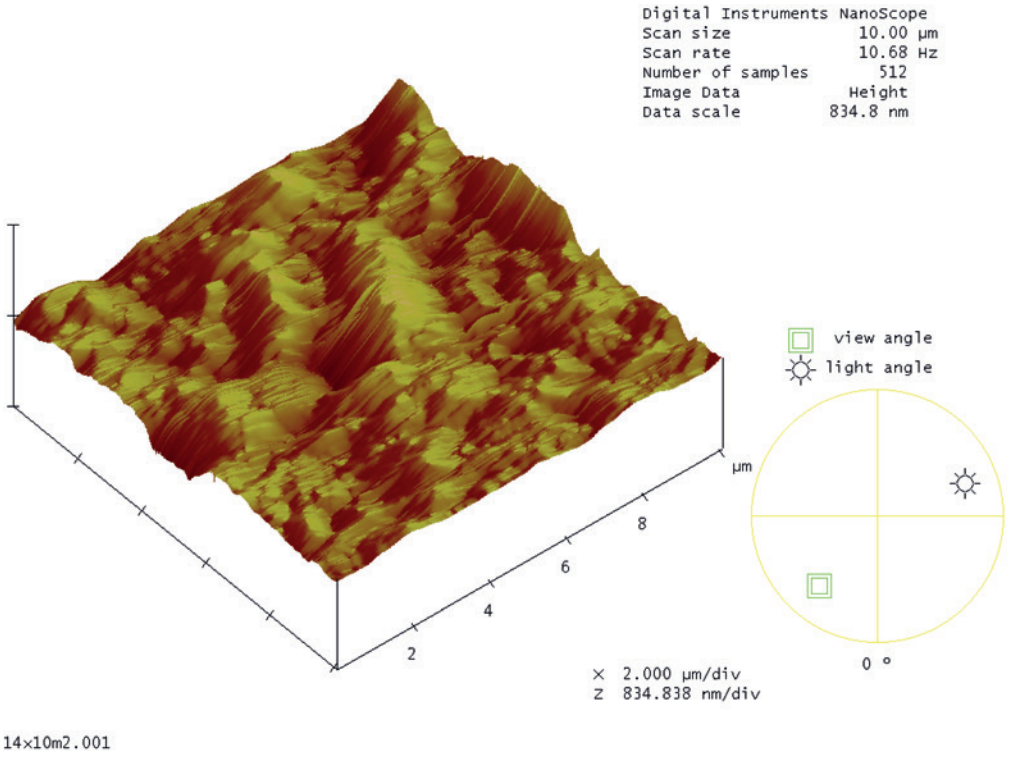

(b)

Fig. 1: AFM photographs of the probertite pellet sample, (a) 2-dimensional view, (b) 3-dimensional view, (c) 2-dimensional 10 × 10 µm flatten view.

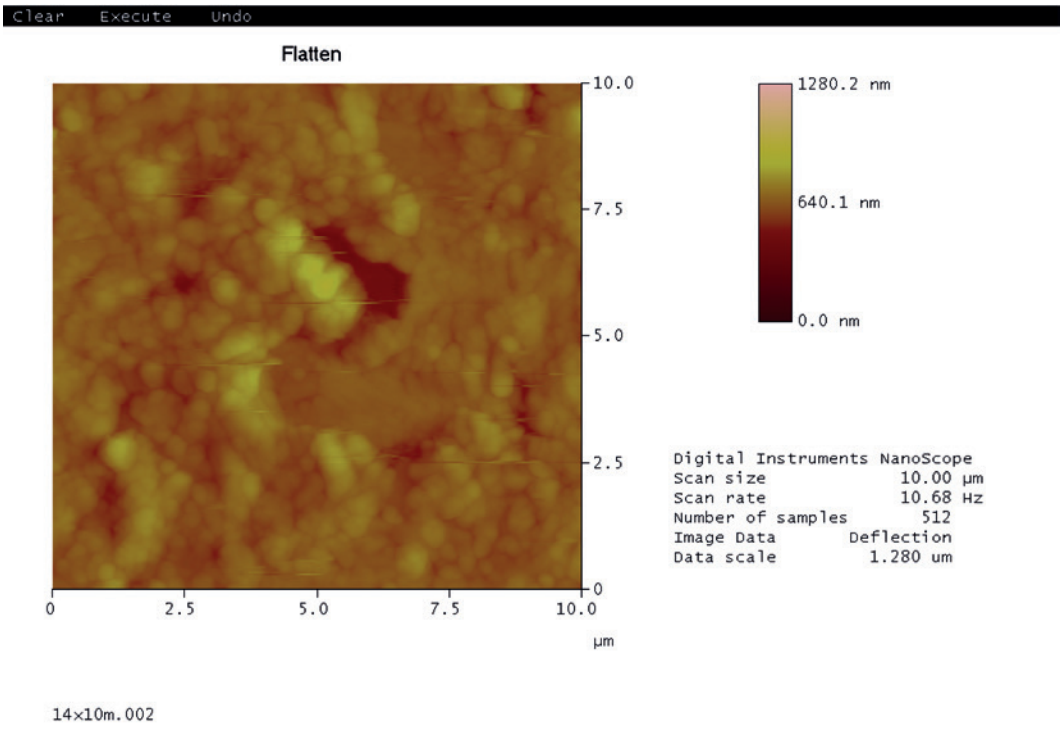

(c)

Fig. 1 (cont.)

where ε_s and ε_∞ are the low and high frequency dielectric constants respectively, τ is the relaxation times constant, and ω is the angular frequency. The ε^* is given by, $\varepsilon^* = \varepsilon' - i\varepsilon''$, where ε' is the relative permittivity or dielectric constant, ε'' is the dielectric loss. Separating the real and imaginary parts of Eq. (1)

$$\varepsilon' = \varepsilon_\infty + \frac{\left(\varepsilon_s - \varepsilon_\infty\right)}{\left(1+\omega^2\tau^2\right)} \tag{2}$$

$$\varepsilon'' = \frac{\left(\varepsilon_s - \varepsilon_\infty\right)\omega\tau}{\left(1+\omega^2\tau^2\right)} \tag{3}$$

$$\tan\delta = \frac{\varepsilon''}{\varepsilon'} = \frac{\left(\varepsilon_s - \varepsilon_\infty\right)\omega\tau}{\left(\varepsilon_s + \varepsilon_\infty\omega^2\tau^2\right)} \tag{4}$$

Many real materials show a deviation from an ideal equation and exhibit a non-Debye dielectric behavior. The non-Debye dielectric response can be described using Cole-Cole, Davidson-Cole and empirical expression proposed by Havriliak-Negami (H-N) [15–18].

The dielectric behavior of the system has been studied over a range of frequency and temperature. Fig. 2 shows the variation of dielectric constant as a function of frequency at different temperatures. Initially, the value ε' is very high. Further, dielectric constant decreases gradually with increasing frequency and showing dispersive behavior at low frequencies. These are characteristic of dielectric materials [19]. From Fig. 2, it is observed that with increase in frequency, ε' decreases and attains to same value at high frequencies. At high frequencies, due to the high periodic reversal of the AC field, there is no charge accumulation at the interface and hence the

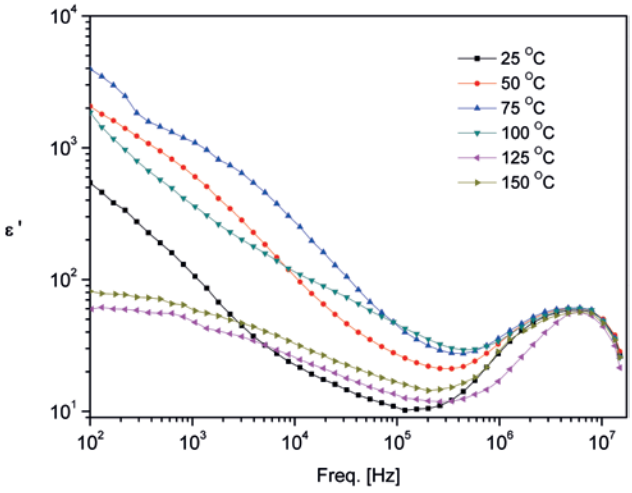

Fig. 2: Frequency dependency of the real part of dielectric constant at different temperatures.

ε' approaches same values, which can be explained in terms of the ion diffusion mechanism. At low frequencies, the charges get accumulated at the interfacial region that lead to a net polarization of the ionic medium result in the formation of space charge region at electrode-electrolyte interface which in turn increases the dielectric constant ε' [20–25]. Since probertite material has a high dielectric constant value in the frequency range of 10^6–10^7, by this situation we have verified that probertite, which exhibits a wide range spectrum variation, has electromagnetic absorption capacity. It reveals the fact that materials which have electromagnetic absorption property can be used as alternative cement additive material.

The dielectric strength is the difference between the dielectric values at minimum and at maximum frequencies. In the impedance spectroscopy technique the dielectric strength $\Delta\varepsilon$ is expressed as

$$\Delta\varepsilon = \varepsilon_0 - \varepsilon_\infty \tag{5}$$

where ε_s and ε_∞ are the minimum and maximum components of the dielectric constant. Figure 2 shows clearly that the temperature of decreases the dielectric strength of the probertite sample. In fact, values of the dielectric strength $\Delta\varepsilon$ deduced from Figure 2, which are given in Table 2. With the temperature, $\Delta\varepsilon$ values decreased approximately from 1996 to 47 in the frequency range (from 100 to 201k Hz). This shows that probertite exhibits high electromagnetic absorption behavior corresponding to the dielectric strength values in the temperature range from 50 °C to 100 °C.

The frequency and temperature dependence of dissipation factor (or dielectric loss tangent) for probertite was demonstrated in Fig. 3 and maximum value variations of ε', tan δ, M', M'' and AC conductivity (σ) with temperature at critical frequencies were shown in Table 3. Fig. 3 designates how dissipation factor becomes different by decreasing measurement temperature of probertite which shifts to higher temperatures with increasing frequencies between 25 °C and 150 °C. The above loss peaks and their

Table 2: Dielectric strength of probertite.

Temperature (°C)	Δε
25	532.07
50	1996.17
75	1932.04
100	1814.77
125	47.70
150	67.02

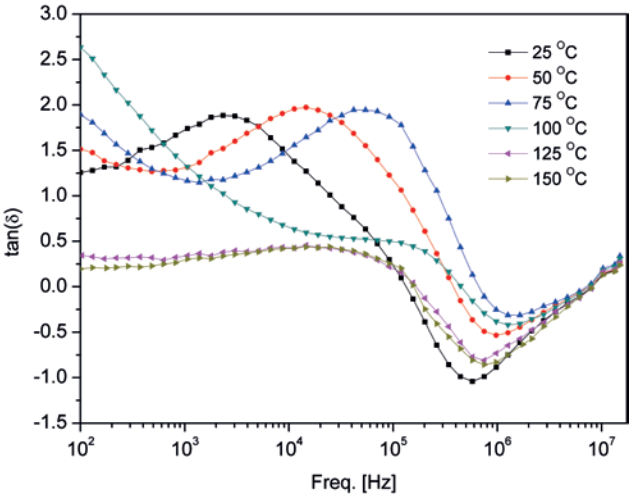

Fig. 3: Frequency dependency of the dissipation factor at different temperatures.

Table 3: Maximum values of probertite as dependent on electrical parameters.

Temperature (°C)	$\varepsilon' \times 10^2$ 100 Hz	tan δ	Modulus $\times 10^{-2}$	Modulus″ $\times 10^{-2}$	Sig′(S/cm) $\times 10^{-5}$
25	5.42	1.88	9.72	3.65	6.08
50	20.68	1.97	4.69	2.10	6.26
75	39.63	1.94	3.44	1.73	7.34
100	18.50	2.63	3.53	1.10	6.69
125	0.707	0.56	8.20	2.02	4.75
150	0.766	4.38	6.64	1.64	5.06

shifts with temperature suggest a dielectric relaxation process [26–27]. The maximum value of tan δ has been determined at 75 °C after the lightning progress. At high temperatures (100 to 150 °C), it has been found that tan δ value falls in spite of increasing frequency in Fig. 3. $\varepsilon' = \varepsilon''/\tan\delta$ is an exact reflection of Eq. (4). While the maximum points in Fig. 3 have the dielectric relaxation effect and the dielectric relaxation frequency points, we have seen that it has increased with temperature and the effect has disappeared in high temperatures.

The complex electric modulus is defined by the reciprocal of the complex permittivity [9]

$$M^* = \frac{1}{\varepsilon^*} = j\omega C_0 Z^* \tag{6}$$

$$M^* = M' + jM'' = j\omega C_0 \left(Z' - jZ''\right) \tag{7}$$

where M^* is the complex modulus, M' is the real and M'' is the imaginary parts of modulus. The complex electric modulus spectrum represents the measure of the

distribution of ion energies or configurations in the structure and it also describes the electrical relaxation and microscopic properties of ionic glasses [28, 29]. The modulus formalism has been adopted as it suppresses the polarization effects at the electrode/electrolyte interface. Hence, the complex electric modulus $M(\omega)$ spectrum reflects the dynamic properties of the sample alone. For parallel combination of RC element, the real and imaginary parts of the modulus. In case of real solid electrolyte, the modulus spectra exhibit a broad and asymmetric non-Debye nature with distribution of relaxation times. In Figs. 4 and 5, the existence of critical frequency determination of the resonance condition that provides electromagnetic absorption property for probertite is shown. As frequency increases the value of M' increases and reaches a maximum constant value of $M_\infty = 1/\varepsilon_\infty$ at higher frequencies for all temperatures. These observations may possibly be related to a lack of restoring force governing the mobility of charge carriers under the action of an induced electric field. This type of behavior supports the conduction phenomena due to long-range mobility of charge carriers [30–32]. In Figs. 4–5, it is seen that the shape of the curves are asymmetric with a long tail extending in the higher frequency region exhibiting non-Debye behavior and it is also observed that the peak relaxation frequency f_{max} shifts towards the higher frequency region with temperature. According to the obtained results, the M'' curves are related to the energy dissipation in the irreversible conduction process and they exhibit a non-exponential character of decay process [33].

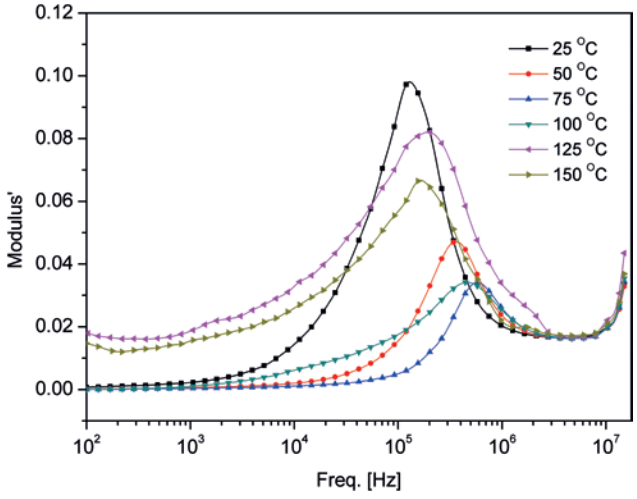

Fig. 4: Frequency dependence of M' at various temperatures.

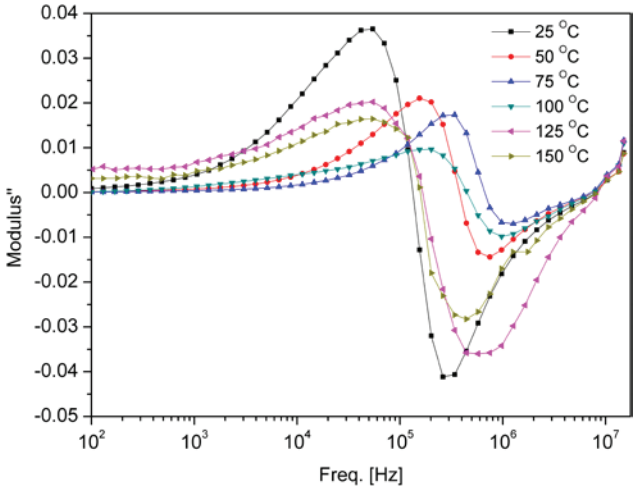

Fig. 5: Frequency dependence of M'' at various temperatures.

As shown in Fig. 6, AC conductivity (σ) increases and makes a maximum at 75 °C for the lower frequencies ($f < 10^5$ Hz), and it starts to decrease at 100 °C. This change is interpreted to be compatible with the $\Delta\varepsilon$ exchange. Also as shown in the inset of Fig. 6, a log-log ($\sigma - f$) graph is plotted for frequencies from 100 to 10^5 Hz, and the highest AC conductivity values are obtained for a temperature of 75 °C. The dependence of the AC conductivity on temperature is given in Fig. 6 according to Arrhenius equation,

$$\sigma = \sigma_o \exp(-E_A / kT) \tag{8}$$

where σ_o is a constant, E_A is the electrical activation energy ($k_B = 8.6173 \times 10^{-5}$ eVK^{-1}). The activation energy of conduction is calculated from the slopes of lines in the graph ln σ_{AC} versus 1000/T for different frequencies [34].

As seen in Table 4, almost all activation energy values are close to zero after $f > 10^5$ Hz, because of resonance

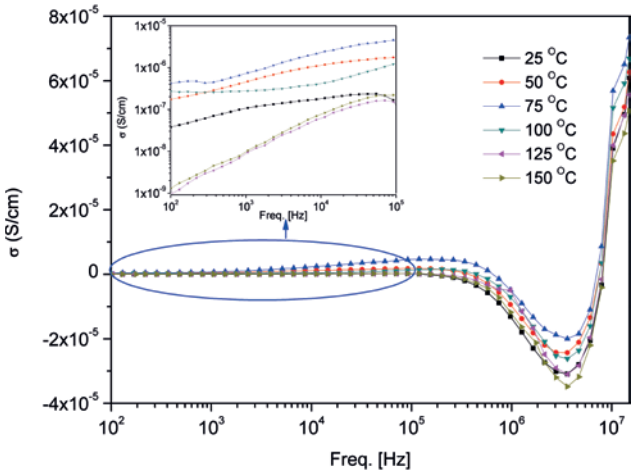

Fig. 6: Frequency dependence of the real part of conductivity at different temperatures.

Table 4: Activation energy values of probertite as dependent on frequency.

Freq. (Hz)	1×10^2	1×10^3	1×10^4	1×10^5	1×10^6	1×10^7	1.5×10^7
$E_A(eV)$ (± 0.01)	0.43	0.45	0.46	0.48	0.058	0.066	0.033

frequency which is in good agreement with dielectric property of probertite and activation energy, which has increasing variation with increasing frequency prior to frequency values in this region. Therefore we can conclude that probertite has electromagnetic absorption property. After this frequency ($f > 10^5$ Hz), conductivity variation deviates from the linear behavior and the activation energy approaches zero. That means when this material is excited with these frequencies, the variation moves away from the linear behavior since the material absorbs the electromagnetic radiation and the material exhibits activation energy such as a conductor.

4 Conclusions

Dielectric spectroscopy and electrical parameters of probertite material were investigated in the broad band frequency range of 100 to 15 MHz. Here from the present study it can be concluded that, electrical modulus of probertite indicates that critical frequency values and resonance condition can ensure electromagnetic absorption capacity and exhibit non-exponential type conductivity relaxation. Critical frequency values of the real part of electrical modulus are changed for probetite with ambient temperatures. It is found 75 °C in the highest frequency (570349 Hz) for the effective industrial applications. These properties can appropriate new broad band absorption capacity for shielding concrete and in different types of special cement additive material. Since probertite exhibits a wide range resonance spectrum in the frequency range of 10^6–10^7 Hz, this reveals electromagnetic absorption property of probertite. As a result of this work, it is suggested that concretes and cements, including probertite materials, could be used practically as a shielding in industrial applications.

Received: November 25, 2013. Accepted: December 26, 2013.

References

[1] V.M. Malhotra, M.P. Kumar, *Pozzolanic and Cementitious Materials*, Gordon and Breach Science Publisher, SA (1996).
[2] M.F. Kaplan, *Concrete Radiation Shielding*, Longman Scientific & Technical, UK (1989).
[3] J.K. Shultis, R.E. Faw, *Radiation Shielding*, ISBN 0-13-125691-2, Prentice Hall, Upper Saddle River, NJ (1996).
[4] I. Akkurt, C. Basyigit, S. Kilincarslan, B. Mavi, *Progress in Nuclear Energy*, **46** (2005) 1–11.
[5] M.H. Kharita, M. Takeyeddin, M. Alnassar, S. Yousef, *Progress in Nuclear Energy*, **50** (2008) 33–36.
[6] M.F. Kaplan, *Concrete Radiation Shielding: Nuclear Physics, Concrete Properties, Design and Construction*, Longman Scientific & Technical, UK (1989).
[7] M.A. Ibrahim, R.A. Rashed, *Nuclear Science Journal*, **35** (1998) 245–250.
[8] A. Mergen, M.H. Demirhan, *International Journal of Mineral Processing*, **90** (2009) 16–20.
[9] J.R. Macdonald, *Impedance Spectroscopy*, John Wiley & Sons, New York (1987).
[10] J.F. Mccann, S.P.S. Badwal, *J. Electrochem. Soc.*, **129**(3) (1982) 551–559.
[11] B. Roling, *J. Non-Cryst. Solids*, **244** (1999) 34–43.
[12] S.P.S. Badwal, *Solid State Ionic Devices*. In: B.V.R. Chowdari and S. Radhakrishna (eds.), World Scientific, Singapore (1988).
[13] J.E. Bauerle, *J. Phys. Chem. Solids*, **30** (1969) 2657–2670.
[14] A. Hooper, *Application of a.c. measurement and analysis techniques to materials research*, AERE-R9757 (1980).
[15] L.L. Hench, J.K. West, *Principles of Electronic Ceramics*. John Wiley & Sons, Singapore (1990).
[16] D.W. Davidson, R.H. Cole, *J. Chem. Phys.*, **19** (1951) 1484.
[17] D.W. Davidson, R.H. Cole, *J. Chem. Phys.*, **19** (1951) 1484–1490.
[18] S. Havriliak, S. Negami, *Polymer*, **8** (1967) 161–210.
[19] S.K. Sinha, S.N. Choudhary, R.N.P. Choudhary, *Mater. Chem. Phys.*, **70** (2001) 296–299.
[20] M.D. Ingram, *Phys. Chem. Glasses*, **28** (1987) 215–234.
[21] C. Liu, C.A. Angell, *J. Non-Cryst. Solids*, **83** (1986) 162–184.
[22] D.L. Sidebottom, P.F. Green, R.K. Brow, *J. Non-Cryst. Solids*, **183** (1995) 151–160.
[23] K.L. Nagi, J.N. Mundy, H. Jain, O. Kanert, G.B. Jollenbeck, *Phys. Rev. B*, **39** (1984) 6169–6179.
[24] S.W. Martin, C.A. Angell, *J. Non-Cryst. Solids*, **83** (1986) 185.
[25] F.S. Howell, R.A. Bose, P.B. Macedo, C.T. Moynihan, *J. Phys. Chem.*, **78** (1974) 639–648.
[26] K. Prabakar, Sa. K. Narayandass, D. Mangalaraj, *Materials Science and Engineering B*, **98** (2003) 225–231.
[27] J.G. Simmons, G.S. Nadkarni, M.C. Lancaster, *J. Appl. Phys.*, **41** (1970) 538–544.
[28] P.B. Macedo, C.T. Moynihan, R. Bose, *Phys. Chem. Glasses*, **13** (1972) 171–179.
[29] V. Provenzano, L.P. Boesch, V. Volterra, C.T. Moynihan, P.B. Macedo, *J. Am. Cream. Soc.*, **55** (1972) 492–496.

[30] K.P. Padmasree, D.K. Kanchan, A.R. Kulkarni, *Solid State Ionics*, **177** (2006) 475.
[31] S. Saha, T.P. Sinha, *Phys. Rev. B*, **65** (2002) 134103–134106.
[32] M. Ram, S. Chakrabarti, *Journal of Alloys and Compounds*, **462** (2008) 214–219.
[33] C.T. Moynihan, L.P. Boesch, N.L. Laberge, *Phys. Chem. Glasses*, **14**(6) (1973) 122–125.
[34] S.E. San, M. Okutan, T. Nyokong, M. Durmuş, B. Ozturk, *Polyhedron*, **13** (2011) 1023–1026.